Intense Bessel femtosecond pulse propagation in dispersive Kerr medium

Zhenming Song (宋振明)[1] and Takashi Nakajima[2*]

[1]*Department and Institute of Physics, School of Science, Tianjin Polytechnic University, Tianjin 300160, China*

[2]*Institute of Advanced Energy, Kyoto University, Gokasho, Uji, Kyoto 611−0011, Japan*

[*]*Corresponding author: t-nakajima@iae.kyoto-u.ac.jp*

Received December 15, 2010; accepted January 16, 2011; posted online June 29, 2011

The performance of intense Bessel femtosecond pulse propagation in dispersive medium is investigated. Water is chosen as the Kerr medium with large dispersion. We find that within the dispersion length, the temporal profile integrated over the beam radius is controlled mainly by dispersion, whereas the spectral profile is nearly undistorted. We also show the energy flow between different transverse parts of the beam, which provides a reservoir for the intense part of the Bessel beam and extends the nonlinear effect length between the pulse and the Kerr medium as we have previously found in argon.

OCIS codes: 320.2250, 320.7110.

doi: 10.3788/COL201109.S10101.

Since the Bessel beam has been proposed to the beam profile family by Durnin *et al.* in 1987[1,2], the non-diffraction property of the Bessel beam has attracted increasing attention in recent years from both the scientific and technological points of view, such as in microfabrication, harmonic generation, and filamentation. Argon (with small dispersion) is usually chosen as the typical Kerr medium in studying the performance of intense femtosecond pulses. We have studied the characteristics of filament and plasma channel formed by Bessel beams in argon in detail[3,4]. In the current work, we choose water (with large dispersion) as the Kerr medium and investigate the performances of intense Bessel femtosecond pulse propagation in this medium. By solving the general nonlinear Schrödinger equation coupled with the electron density evolution equation[5,6], we reveal the in-depth characteristics of intense Bessel beam propagation in a dispersive medium.

While in argon, dispersion is too small to play an obvious role during propagation for short distance. For the Kerr medium with large dispersion, the contribution of dispersion should not be neglected. Sometimes, it may not only broaden the pulse but also lead to pulse splitting[7]. For the simulation in water, since the intensity we calculated is always in the multiphoton ionization domain, we used the simplified multiphoton ionization model[6,8]. The coefficients for water that we considered are: central wavelength $\lambda_0 = 800$ nm, density of neutral atoms $\rho_{\rm nt} = 6.68 \times 10^{28}/{\rm m}^3$, linear refractive index $n_0 = 1.334$, nonlinear refractive index $n_2 = 4.1 \times 10^{-20}$ m^2/W, the second order dispersive coefficient $k'' = 2.48 \times 10^{-26}$ s^2/m, ionization potential $U_i = 6.5$ eV, the number of photons $K = 5$ required for multiphoton ionization, MPI coefficient reads as $\sigma_K = 1.2 \times 10^{-72}$ m^{10}/(s·W^5) (which corresponds to $\beta_K = 1 \times 10^{-61}$ m^7/W^4), and momentum transfer collision time $\tau_{\rm c} = 3$ fs. The cross-section for inverse bremsstrahlung follows the Drude mode[9] and reads as $\sigma = \dfrac{k_0 e^2}{n_0^2 \omega_0^2 \varepsilon_0 m} \dfrac{\omega_0 \tau_{\rm c}}{1 + \omega_0^2 \tau_{\rm c}^2}$, where e is the electron charge and m is the electron-hole reduced mass for gas or condensed dielectric medium. For water, m equals half of the mass of electrons $m_{\rm e}$, i.e., $m = 0.5\, m_{\rm e}$. In addition, $k'' = 2.48 \times 10^4$ fs^2/m, which means the dispersion length $L_{\rm D} = 1.31$ cm. The propagation distance is set as 5 cm, and we have also chosen 30-fs, 100-μm Bessel beam as the incident pulse, unless otherwise specified.

First, we investigated the evolution of the temporal profiles. We plotted the temporal profiles integrated over the beam radius at different propagation distances for different incident peak powers and beam diameters (see Figs. 1(a)–(f)). The peak power was measured by the self focusing critical power $P_{\rm cr} = \lambda^2/2\pi n_0 n_2$. The

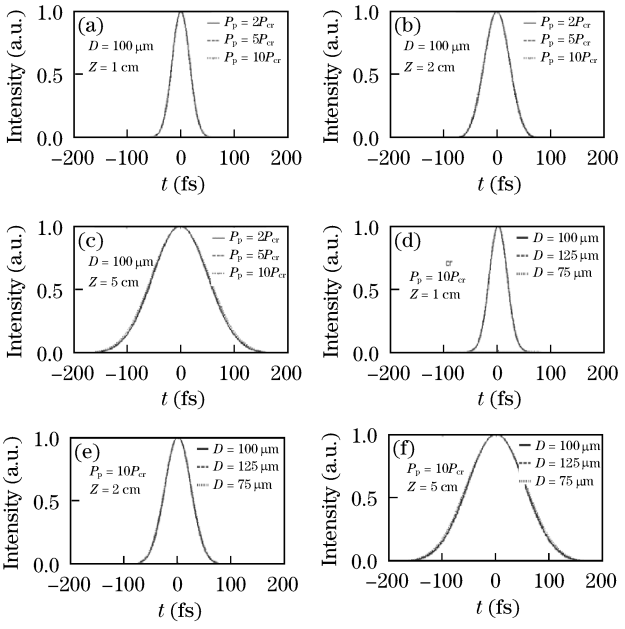

Fig. 1. Temporal profiles integrated over the beam radius of an incident pulse with a diameter of 100 μm with different peak powers at Z = (a) 1, (b) 2, and (c) 5 cm, and a $10P_{\rm cr}$ peak power with different diameters at Z = (d) 1, (e) 2, and (f) 5 cm.

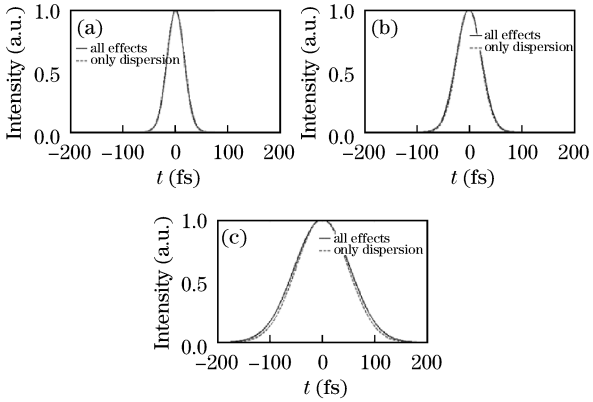

Fig. 2. Temporal profiles integrated over the beam radius of a $10P_{cr}$ peak power incident pulse with a diameter of 100 μm with all the effects and only dispersion taken into account at z = (a) 1, (b) 2, and (c) 5 cm.

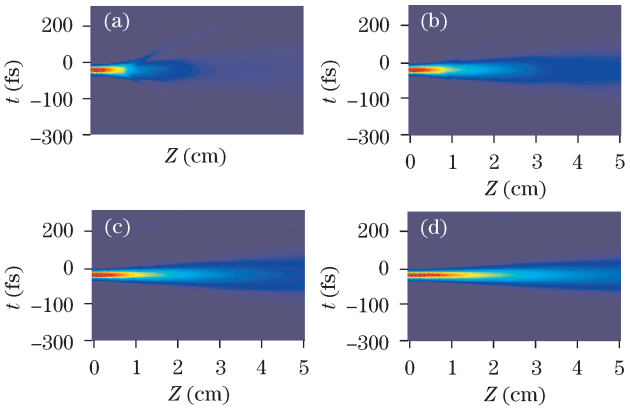

Fig. 3. Evolution of temporal profiles integrated over the beam radius within (a) 100, (b) 200, (c) 500 μm, and (d) the whole space as a function of the propagation distance for a $10P_{cr}$ peak power incident pulse with a diameter of 100 μm.

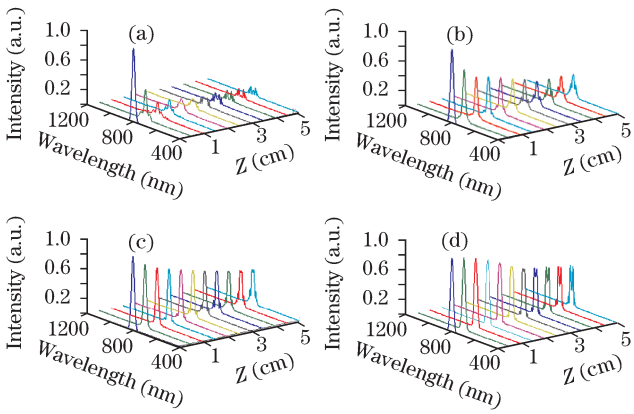

Fig. 4. Evolution of the spectral profiles integrated over the beam radius within (a) 100 μm, (b) 200 μm, (c) 500 μm, and (d) the whole space as a function of the propagation distance for $10P_{cr}$ peak power incident pulse with a diameter of 100 μm.

temporal profiles were normalized by themselves. Usually, the temporal profiles with different peak powers

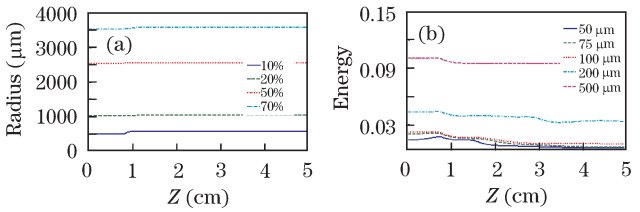

Fig. 5. (a) Radii containing different energies and (b) energy contained within different radii as functions of the propagation distance for $10P_{cr}$ peak power incident pulse with a diameter of 100 μm.

and beam diameters are nearly identical at the same propagation distance, and only dispersion contributes to the distortion of the temporal profiles integrated over the beam radius. To prove this conclusion, we compared the temporal profiles of all linear and nonlinear effects with those of only the dispersion effect taken into account for the $10P_{\rm cr}$ peak power, 100-μm diameter incident pulses at different distances. They are shown in Figs. 2(a)−(c). Figures 2(a)−(c) further prove the conclusion that the temporal profiles of the Bessel beam integrated with the beam radius are only affected by dispersion. To make this conclusion more specific, we state that it is tenable with the dispersion length $L_{\rm D}$, whereas it begins to deviate beyond $L_{\rm D}$.

We also investigated the evolution of the temporal and spectral profiles integrated with different radii during the propagation. They are shown in Figs. 3 and 4, respectively. Within the dispersion length, when the spatial integration range increased, the temporal profiles converged to the profile controlled by dispersion, whereas the spectral profiles converged to the original (see Figs. 3 and 4). This tendency comes from the contribution of the peripheral part of the beam, which has comparable energy and suffers small distortion.

After studying the evolution of temporal and spatial profiles, we investigated the energy flow between different transverse parts of the beam. We plotted the radii containing different energies and energy contained within different radii as functions of the propagation distance, respectively (see Figs. 5(a) and (b)). The reservoir effect for radius larger than 100 μm was very small, but when we reduced the radius (for 75 and 50 μm), the reservoir effect became obvious (see Fig.5 (b)). The reservoir effect distance for water was also very short.

In conclusion, we choose water as the large dispersive Kerr medium in order to investigate the temporal and spectral propagation performances in the dispersive Kerr medium through theoretical simulations. We show that within dispersion length, the temporal profile integrated over the beam radius is controlled by dispersion, and that the spectral profile integrated over the beam radius is nearly undistorted. We also conduct energy flux diagnostic to show the energy flow between different transverse parts of the Bessel beam. Based on the observation, the energy flowing between different transverse parts of the beam serves as an energy reservoir and extendes the nonlinear effect between the pulse and the Kerr medium.

References

1. J. Durnin, J. J. Miceli Jr., and J. H. Eberly, Phys. Rev. Lett. **58,** 1499 (1987).
2. J. Durnin, J. Opt. Soc. Am. A **4,** 651 (1987).
3. Z. Song, Z. Zhang, and T. Nakajima, Opt. Express **17,** 12217 (2009).
4. Z. Song and T. Nakajima, Opt. Express **18,** 12923 (2010).
5. G. P. Agrawal, *Nonlinear Fiber Optics* (Academic, San Diego, 1995).
6. M. Mlejnek, E.M. Wright, and J. V. Moloney, Phys. Rev. E **58,** 4903 (1998).
7. J. E. Rothenberg, Opt. Lett. **17,** 583 (1991).
8. P. Polesana, M. Franco, A. Couairon, D. Faccio, and P. Di Trapani, Phys. Rev. A **77,** 043814 (2008).
9. E. Yablonovitch and N. Bloembergen, Phys. Rev. Lett. **29,** 907 (1972).